Chemical Science

ROYAL SOCIETY OF CHEMISTRY

EDGE ARTICLE

Check for updates

All publication charges for this article have been paid for by the Royal Society of Chemistry

Liposome fusion with orthogonal coiled coil peptides as fusogens: the efficacy of roleplaying peptides†

Geert A. Daudey, [ID] ‡[a] Mengjie Shen,[a] Ankush Singhal, [ID] [a] Patrick van der Est,[a] G. J. Agur Sevink, [ID] [a] Aimee L. Boyle [ID] [b] and Alexander Kros [ID] *[a]

Biological membrane fusion is a highly specific and coordinated process as a multitude of vesicular fusion events proceed simultaneously in a complex environment with minimal off-target delivery. In this study, we develop a liposomal fusion model system with specific recognition using lipidated derivatives of a set of four *de novo* designed heterodimeric coiled coil (CC) peptide pairs. Content mixing was only obtained between liposomes functionalized with complementary peptides, demonstrating both fusogenic activity of CC peptides and the specificity of this model system. The diverse peptide fusogens revealed important relationships between the fusogenic efficacy and the peptide characteristics. The fusion efficiency increased from 20% to 70% as affinity between complementary peptides decreased, (from $K_F \approx 10^8$ to 10^4 M^{-1}), and fusion efficiency also increased due to more pronounced asymmetric role-playing of membrane interacting 'K' peptides and homodimer-forming 'E' peptides. Furthermore, a new and highly fusogenic CC pair (E$_3$/P1$_K$) was discovered, providing an orthogonal peptide triad with the fusogenic CC pairs P2$_E$/P2$_K$ and P3$_E$/P3$_K$. This E$_3$/P1$_k$ pair was revealed, *via* molecular dynamics simulations, to have a shifted heptad repeat that can accommodate mismatched asparagine residues. These results will have broad implications not only for the fundamental understanding of CC design and how asparagine residues can be accommodated within the hydrophobic core, but also for drug delivery systems by revealing the necessary interplay of efficient peptide fusogens and enabling the targeted delivery of different carrier vesicles at various peptide-functionalized locations.

Introduction

Membrane fusion is key for cellular survival as it facilitates the formation and downstream processing of transporter vesicles, intracellular endosomes and extracellular synaptic vesicles.[1] The fusion of membranes is largely governed by SNARE proteins, a protein family identified by a well conserved tetrameric coiled coil (CC) motif with 60–70 amino acids per α-helix.[2–4] SNARE proteins fulfil a multifaceted role in the fusion mechanism; they signal the position where fusion should occur and they provide (part of) the necessary force to overcome multiple energy barriers of merging initially stable membranes.[5] Besides the study of the role of SNARE proteins in

the natural fusion process, a variety of simpler synthetic fusogens have been developed to mediate membrane fusion. Such fusogens are based on DNA,[6–12] PNA,[13–15] peptides,[16–21] or small molecules.[22–28] These model systems rely on strong binding interactions between the membrane tethered molecules, forcing opposing liposomes into close proximity with concomitant fusion. Our previous efforts in this field yielded peptide-based fusogens, the heterodimeric CC pair E$_3$ and K$_3$ (with the amino acid sequences (EIAALEK)$_3$ and (KIAALKE)$_3$ respectively). The peptides were functionalized with a polyethyleneglycol (PEG) based spacer and a lipid anchor for membrane immobilization. Previously, we found that the efficiency of these fusogens strongly depends on the concerted influences of membrane anchor type,[29] PEG-spacer length,[30] and peptide length and orientation,[31–34] with cholesterol–PEG$_4$–E$_4$/K$_4$ being very efficient both *in vitro* (fusion of liposomes with GUVs) and *in vivo* (liposome–cell fusion).[35–38] We identified defined, separate roles of E$_3$ and K$_3$ which are crucial for efficient fusion; Peptide K$_3$ promotes the formation of lipid protrusions by spontaneous membrane insertion, while peptide E$_3$ acts as a handle to enable the docking of opposing liposomes.[39–43]

*a*Supramolecular and Biomaterials Chemistry, Leiden Institute of Chemistry, Leiden University, P.O. Box 9502, 2300 RA Leiden, The Netherlands. E-mail: a.kros@chem.leidenuniv.nl

*b*Macromolecular Biochemistry, Leiden Institute of Chemistry, Leiden University, P.O. Box 9502, 2300 RA Leiden, The Netherlands
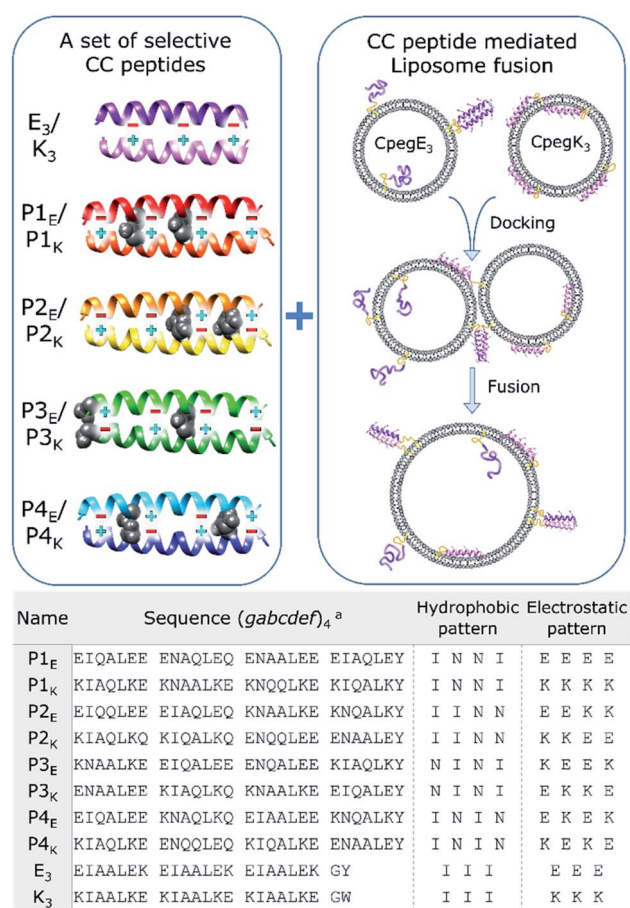
Most model systems, including ours, are based on a single complementary recognition unit,[44] and are thus only a limited mimic of the targeted specificity of the SNARE protein family. Therefore, one of the remaining challenges in the field of artificial membrane fusion is to mimic the specificity of biological fusion processes. Specific recognition and fusion of liposomes has been demonstrated using DNA- and PNA-based fusogens.[12,13] However, these systems only showed efficient fusion at 50 °C, making this approach impractical for biological applications.

In recent years, several sets of orthogonal CC peptides have been developed.[45–53] We hypothesized that specific recognition in a liposomal fusion assay could be achieved using such orthogonal CC peptides as fusogens. We selected a set of orthogonal CC peptides that fulfilled our desired criteria, namely that the peptides should be highly selective for their designed partner, the T_m of the heterodimer should be above 37 °C in order for this system to be suitable for biological applications, and the peptides should not be derived from natural peptides or proteins, to minimize any potential crosstalk if this system is applied *in vitro* or *in vivo*. We characterized the peptides and assessed their ability to facilitate liposomal fusion using circular dichroism (CD) spectroscopy, fluorescence-based quantitative content mixing assays and molecular dynamics (MD) simulations. Through analyzing this set of orthogonal fusogenic peptides we were able to illustrate the following: (1) fusion only occurs between liposomes bearing complementary peptides; (2) structure–fusogenic activity relationships of the CC pairs are defined by their helical propensities, CC binding strengths, and membrane interactions, and; (3) membrane tethering of (CC) peptides affects their preferred conformations and intermolecular interactions as we demonstrated previously for the E_3/K_3 pair.[30,39,40] Furthermore, we found a significant cross-pair interaction ($E_3/P1_K$), which was subjected to MD simulations and the resulting model analyzed to uncover the core packing. We discovered a shifted heptad repeat register, which we hypothesize occurs to compensate for the inclusion of two asparagine residues. Through this study, we have also expanded the range of available CC fusogens opening up avenues for fusion cascades and a variety of biological applications, in addition to gaining fundamental insights into the accommodation of mismatched 'core' asparagine residues in coiled coils.

Design of the study

Several sets of orthogonal CC peptides have been reported to date, but they must meet several requirements to be useful candidates for a peptide-mediated fusion system. We considered only orthogonal heterodimeric peptide sets as fusogens because fusion should only occur between transporter vesicles and target membranes, and homomeric CC interactions would most likely inhibit fusion due to strong homo-oligomerization of membrane immobilized peptides.[45,46] To further reduce off-target fusion, any cross-pair interaction should have a T_M below 37 °C which eliminated sets developed by Aili[47] and Mason,[48,49] although these peptides could be highly fusogenic.

Conversely, the T_M of the desired CC interactions should not be lower than 25 °C which would hamper fusion even at room temperature, dismissing one more set published by Woolfson.[50] Also, the candidate peptides should not bind to biological targets to avoid unintended interactions, as could be the case with the set of CC peptides derived from Leucine zipper DNA-binding peptides published by Keating.[51] Additionally, the peptide set developed by Kennan[52] was limited to only two orthogonal peptide pairs due to the incorporation of just one polar bridge (Asn–Asn or Asp–Arg) in the hydrophobic core to direct selective CC formation. In 2011, these issues were addressed, or circumvented, in the CC peptide design of Jerala, by using a four heptad repeat with four buried Asn residues per pair (dubbed here Pn_{EK} or Pn_E/Pn_K with $n = 1–4$).[53] Their design choices resulted in significant and selective CC interactions ($T_M \geq 37$ °C) with only weak cross-pair interactions and four potential CC pairs. In general, this makes the set of Jerala

Name	Sequence (gabcdef)₄ [a]	Hydrophobic pattern	Electrostatic pattern
$P1_E$	EIQALEE ENAQLEQ ENAALEE EIAQLEY	I N N I	E E E E
$P1_K$	KIAQLKE KNAALKE KNQQLKE KIQALKY	I N N I	K K K K
$P2_E$	EIQQLEE EIAQLEQ KNAALKE KNQALKY	I I N N	E E K K
$P2_K$	KIAQLKQ KIQALKQ ENQQLEE ENAALEY	I I N N	K K E E
$P3_E$	KNAALKE EIQALEE ENQALEE KIAQLKY	N I N I	K E E K
$P3_K$	ENAALKE KIAQLKQ KNAALKE EIQALEY	N I N I	E K K E
$P4_E$	EIQALEE KNAQLKQ EIAALEE KNQALKY	I N I N	E K E K
$P4_K$	KIAQLKE ENQQLEQ KIQALKE ENAALEY	I N I N	K E K E
E_3	EIAALEK EIAALEK EIAALEK GY	I I I	E E E
K_3	KIAALKE KIAALKE KIAALKE GW	I I I	K K K

Scheme 1 Schematic overview of orthogonal CC peptide pairs combined with a peptide mediated liposomal fusion assay. Partner selectivity for P-peptides is obtained by placing two Asn–Asn pairs (black space-filling) at varying a-positions in the hydrophobic core and unique electrostatic patterns at e and g positions (plus and minus signs). Peptide functionalized liposomes are initially separated, and liposomes dock and fuse due to CC formation of complementary peptides. Used peptide sequences are described in the table, linker structures are available in the ESI.† [a]The heptad repeat starts with position g to increase g–e′+1 interactions.

a priori the most useful candidate to be considered as fusogens in a partner-specific liposomal fusion model system. Functional membrane tethered complementary recognition motifs as well as soluble N-acetylated peptides were synthesized (Scheme 1, Tables S1, S2, and Fig. S1–S3†). The Pn_{EK} four-heptad repeat sequences were taken from Gradišar *et al.*,[53] and the E_3/K_3 sequences were used previously in our membrane fusion studies.[30] The reported Pn_{EK}–peptide sequences have an N-terminal Gly-Ser-Pro-Glu-Asp (GSPED) sequence which acts as an N-terminal capping motif. Since our E_3/K_3 peptide fusogens do not possess such a motif, we omitted it from the sequences used for this study. The peptide–peptide and peptide–membrane interactions of acetylated and lipidated peptides were analyzed by temperature- and concentration-dependent CD spectroscopy, revealing a significant cross-pair CC interaction between E_3 and $P1_K$. The fusogenic efficiency of all CC peptide pairs as well as off-target combinations was investigated using a content mixing assay. The extraordinarily fusogenic hybrid CC pair $E_3/P1_K$ is further studied *in silico* to understand the structural implications of two asparagine (Asn)–isoleucine (Ile) mismatches within the hydrophobic core. Analysis of relationships between peptide secondary structure and amphipathicity, peptide-membrane interactions and fusogenic efficacy of complementary peptides provided further insight into the mechanism of peptide mediated fusion of liposomes, with major effects being peptide binding affinity and peptide–membrane interactions.

Results and discussion

Characterization of peptide complex formation

The quaternary structure and related partner specificity of the Pn_{EK} pairs and E_3/K_3 was probed using CD spectroscopy.[54,55] Equimolar mixtures of all peptide–peptide combinations with a final concentration of 200 μM were measured in PBS buffer with a pH of 7.4 and their helical content (θ_{222} value) was analyzed.[56] The obtained spectra (Fig. 1A and S4†) show that individual peptides adopt either random coil or α-helical structures under these conditions, in agreement with literature.[53] Spectra of peptide mixtures were compared to the averaged spectra of the individual peptides and found helicity deviations (% ΔH) were used to identify heteromeric peptide–peptide interactions (Tables S3–S5†). Typical CC spectra with minima around θ_{222} nm and θ_{208} nm and a % ΔH between 30% and 60%, were found for the five designed peptide pairs but also for the hybrid pair of $E_3/P1_K$, which we will discuss later in more detail. Only three weak cross-pair interactions were found ($P1_E/K_3$, $P3_E/P1_K$, and $E_3/P3_K$; % $\Delta H \approx 15\%$) while all other peptide combinations showed negligible intermolecular interactions (% $\Delta H \leq 10\%$). These observations agree with the reported monomeric and heterodimeric oligomer states of individual peptides and designed pairs respectively, using size exclusion chromatography.[53]

Next, thermal unfolding curves of the six CC peptide pairs: $Pn_{E/K}$, E_3/K_3, and $E_3/P1_K$, were recorded at various equimolar concentrations (Fig. 1B, C, S5, and Table S6†). The obtained data was analyzed by the Matlab package *FitDis!*[57] which
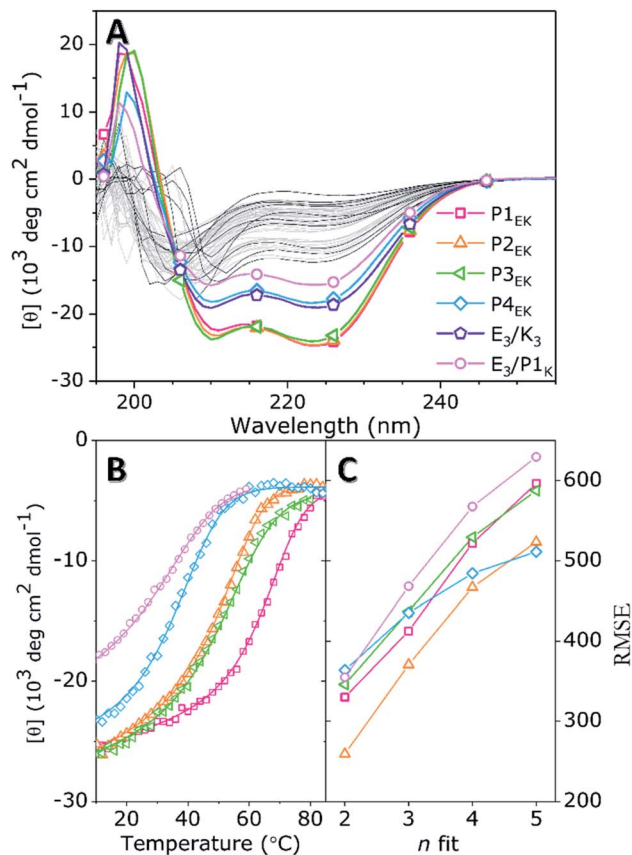

Fig. 1 (A) CD spectra of individual peptides (black, unlabelled) and the found six CC pairs (multicolor) in pure PBS. All other off-target combinations are shown in light grey illustrating the absence of significant spectral deviations. (B) Thermal unfolding curves of designed pairs $P1_{EK}$, $P2_{EK}$, $P3_{EK}$, and $P4_{EK}$, and the found hybrid pair $E_3/P1_K$ are shown. Best fits (lines) of experimental data (dots) are obtained using *FitDis!*. (C) RMSE of best fits for oligomer state n shows that the unfolding is best described for $n = 2$, demonstrating a heterodimeric CC interaction for all peptide pairs. [Total peptide] = 200 μM, PBS (20 mM PO_4^{3-}, 150 mM NaCl) pH 7.4, at 20 °C.

quantifies peptide complex formation by fitting both oligomer state and thermodynamics of folding to concentration-dependent thermal unfolding curves. This yielded the thermodynamic parameters shown in Table 1. The fitting procedure demonstrated the heterodimeric binding mode of all CC peptide pairs, because the root mean square error (RMSE) of best fits showed a minimum at $v_1 + v_2 = 2$ in all cases. Although all Pn_{EK} pairs share similar designs and heterodimeric binding modes, CC interactions differ vastly in terms of thermodynamic parameters. The strongest interaction at 200 μM was found for the $P1_{EK}$ peptide pair, with a T_M of 63 °C and a K_F of 7.6×10^7 M^{-1}. CC pairs $P2_{EK}$ and $P3_{EK}$ have comparable temperature stabilities and affinities ($T_M \approx 50$ °C, $K_F \approx 1.5 \times 10^6$ M^{-1}) and are one order of magnitude weaker compared to $P1_{EK}$. As expected, the $P4_{EK}$ pair showed the weakest interaction of the designed CC pairs and unfolded at 37 °C ($K_F = 1.3 \times 10^5$ M^{-1}). The folding constant of the newly discovered hybrid peptide pair $E_3/P1_K$, 2.3×10^4 M^{-1}, is even three orders of magnitude lower than the value found for the strongest pair $1_E/1_K$.

Table 1 Thermodynamic parameters at 25 °C for Pn_{EK}, $E_3/P1_K$ and E_3/K_3 CC pairs[1]

CC pair	ΔG_{25}, kJ mol^{-1}	ΔH_{25}, kJ mol^{-1}	ΔS_{25}, J mol^{-1} K^{-1}	K_F, M^{-1}
$P1_{EK}$	45.0 ± 2.6	145 ± 23	336 ± 72	$7.6 \pm 4 \times 10^7$
$P2_{EK}$	35.5 ± 1.8	116 ± 9.3	269 ± 27	$1.7 \pm 0.2 \times 10^6$
$P3_{EK}$	35.0 ± 1.8	132 ± 11	325 ± 33	$1.4 \pm 0.2 \times 10^6$
$P4_{EK}$	29.1 ± 1.5	144 ± 10	387 ± 29	$1.3 \pm 0.1 \times 10^5$
$E_3/P1_K$	24.9 ± 1.2	112 ± 5.7	292 ± 15	$2.3 \pm 0.1 \times 10^4$
E_3/K_3[a]	41.4	89.7	162	1.8×10^7

[a] Data taken from Rabe *et al.*[57] Errors obtained by *FitDis!*, and a 5% deviation in peptide concentration.

Comparison of Pn pairs with E_3/K_3 showed similar binding strengths for $P1_{EK}$ and E_3/K_3 ($K_F = 1.8 \times 10^7$ M^{-1}). Since both pairs have equal charge patterns, destabilization of the hydrophobic core of $P1_{EK}$ by two a–a′ Asn pairings is balanced by an additional heptad repeat. Secondly, omission of Jerala's helix stabilizing SPED-G modifications at peptide termini did not influence partner-specificity but had a particular effect on the helicity and T_M of $P1_{EK}$ (% $\Delta H \approx -10$; $\Delta T_M \approx -20$ °C) and $P3_{EK}$ (% $\Delta H \approx +10$; $\Delta T_M \approx +10$ °C).[53] It is surprising that omission of a helix stabilizing N-terminal SPED sequence can have opposite effects on the stability of different CC pairs, depending on the sequence. The counterintuitive positive ΔT_M found for $P3_{EK}$ can only be explained by the sequence, since all other parameters are the same. The N-termini of $P3_{EK}$ differ from the N-termini of the other pairs; the first a-position residues are not the usual Ile but buried polar Asn instead. The omission of the charged SPED tetrapeptide could result in a stronger Asn–Asn hydrogen bonding, enhancing the CC interaction. Conversely, the known tendency of highly charged amphiphilic peptides to fray at chain ends is reduced by the addition of the helix stabilizing SPED tetrapeptide as is clearly visible for $P1_E$ and $P1_K$.[40,58,59]

The found T_M deviations between different pairs agreed with sequence – T_M trends published by Mason in 2017.[49] They developed an advanced algorithm (qCIPA) to predict melting temperatures of dimeric CC peptides. However, the predicted T_M values showed significant deviations from experimental values presumably because there is still too little experimental data available to make reliable predictions for sequence context, *i.e.*, significant long-range neighboring effects. Notwithstanding this lack of data, some long-range core and electrostatic effects could be described that correlate well with our findings; for instance, for pairings at a–a′ positions in the hydrophobic core, a NN–II–NN–II pattern was more stable compared to an II–NN–II–NN packing ($\Delta T_M \approx 20$ °C). We observed a ΔT_M of 13 °C for the two pairs in our set with these patterns, resp. $P3_{EK}$ and $P4_{EK}$. Regarding electrostatic interactions, they found that pairs with uniform charge patterns (*i.e.*, same charge at e–e+1 or g–g+1 residues) usually have a higher T_M due to increased inter-molecular attraction between both helices. Our peptide set shows a similar overall trend: the $P1_{EK}$ pair has a uniform charge pattern and showed the highest T_M; $P2_{EK}$, $P3_{EK}$ and $P4_{EK}$ have incremental charge alterations in their electrostatic pattern which correlates well with the found decreases in T_M. The experimental data of our CC peptides can

thus be used to further train and improve T_M predictive algorithms.

CC formation of the hybrid $E_3/P1_K$ peptide pair

The quaternary structure of the unexpected hybrid peptide interaction of $E_3/P1_K$ was investigated with MD simulations and the thermodynamic data was validated with known structures/ deviations. From a design perspective, CC formation between P-peptides and E_3 or K_3 is penalized *via* unfavorable Asn–Ile pairing in the hydrophobic core, as shown in Fig. 2A. However, both $P1_K$ and E_3 have a uniform charge distribution (either lysines or glutamic acids at all e–e^{+1} and g–g^{+1} positions) and are therefore very prone to intermolecular electrostatic interactions. Despite the dedication to understanding the effects of buried polar residues in CC assemblies,[60–65] there is only thermodynamic data available for buried solitary Asn residues.
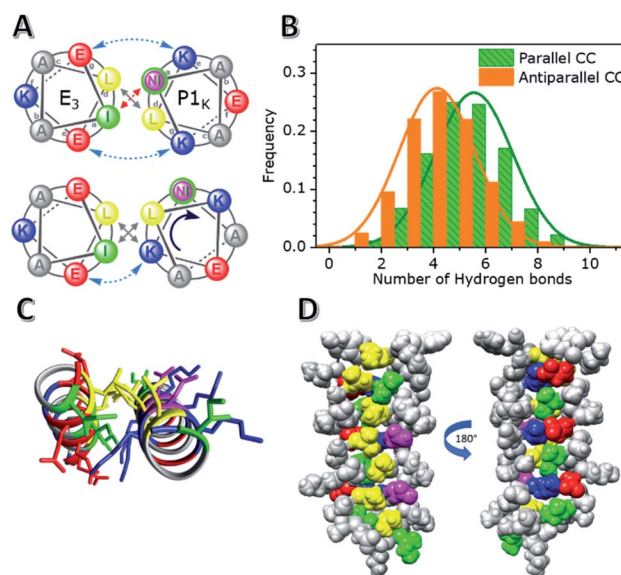

Fig. 2 Results of MD simulations of the hybrid CC pair $E_3/P1_K$. (A) Helical wheels of the second heptad illustrate designed and found CC conformations of $E_3/P1_K$. (B) Average number of established H-bonds between Asn-residues and water molecules for parallel and antiparallel CC conformations. (C) The N-to-C terminal view of the CC formation with a, d, e, g positions visualized. (D) CC side-views showing knobs-into-holes packing and Lys–Glu hydrogen-bonding. Colour guide: Leu (yellow), Ile (green), Lys (blue), Glu (red) and Asn (purple).

Vinson found that the penalty in binding energy for a mismatched a-positional Asn–Ile pairing, which occurs in an assumed $E_3/P1_K$ CC formation, is close to 2 kcal mol^{-1}.[66,67] We found a binding strength difference ($\Delta\Delta G_{37}$) around 4.7 kcal mol^{-1} between $P1_E/P1_K$ or the mismatched pair $E_3/P1_K$. This value correlates very well with a double Asn–Ile mismatch and the shorter three heptad repeat of E_3.

However, MD simulations painted a different picture of the heterodimeric interaction. Two different CC configurations were analyzed: a parallel CC conformation and an antiparallel CC conformation. The parallel conformation was found to be the most stable conformation, highlighted by the switching of the initial antiparallel conformation to a parallel conformation during the 0.6 μs simulation (Fig. S15†). Surprisingly, regardless of the initial CC configuration, both Asns were not buried in the hydrophobic core but interacted with, on average, 5 solvent molecules, as shown in Fig. 2 and S16.† Asn solvation was enabled by a rotation of the $P1_K$ helix by 50° while maintaining the helical pitch, thereby incorporating the relatively hydrophobic g position Lysine residues into the hydrophobic core, as shown in Fig. 2A. The designed Lys–Glu electrostatic interactions are still stabilizing the CC formation on one side of the helix, but they are broken on the other side of the hydrophobic core due to the rotation of the helix. This rotation resulted not only in a change in the heptad repeat register, but also revealed that the Lys residues participated in the knobs-into-holes (KIH) packing of the hydrophobic core, as revealed by SOCKET[68] (a full analysis is available in the ESI†). In short, the rotation of $P1_K$ and the seven-amino acid length difference between E_3 and $P1_k$ caused a shift in the heptad repeat of $P1_K$ from 'KNAALKE' to 'ALKEKNA' (*gabcdef*), presumably to accommodate the two mismatched Asn residues, which were designed to be at position a. Due to this shift these residues are now at the solvent exposed e position, which allows them to make stabilizing hydrogen bonds with water molecules. The two remaining Ile residues of $P1_K$ thus also moved into the solvated e position but only Ile 2 becomes solvent exposed, and Ile 23 fits loosely between two Leucine residues. Therefore, the CC conformation appears to prefer one solvent exposed Ile residue and d positional Lys residues over two unpaired, buried a position Asn residues. This arrangement would also explain the negligible CC interaction of the oppositely charged hybrid pair, $P1_E/K_3$, (% ΔH of only 13%) because a similar tight knobs-into-holes packing would lead to d positional Glu residues which are far less hydrophobic than Lys residues. Thus, although this hybrid mismatched CC pair $E_3/P1_K$ does indeed possess the type of KIH packing one would expect for dimeric CCs, the MD simulations suggest an interesting shift of the heptad repeat assignment of $P1_K$ leading to d position Lys,[64] a position Leu, and e position Ile/Asn residues. A parallel dimeric CC conformation with this particular pattern is unprecedented to our knowledge.[68]

Structure of membrane tethered peptides

Membrane immobilized peptides experience a much higher local concentration than solvated peptides; for example, the

Table 2 Apparent concentration of membrane embedded peptides at 1 mol% functionalization

Peptide	Length (nm)^a	App. conc. (μM)^b
CPeg$_4$ (P)	5.3	3593
CPeg$_{12}$ (P)	8.4	2530
CPeg$_8$ (E_3/K_3)	6.2	3208
Solvation shell^c	11.08	2000

^{a} Calculation of peptide length available in ESI. ^{b} Apparent peptide concentration of membrane embedded peptides in a solvation layer around the liposomal membrane with a thickness equal to the peptide length. ^{c} The volume of a layer with a thickness of ±22 nm centered at the liposomal membrane gives a 2 mM peptide concentration.

standard 1 mol% peptide functionalization of liposomes (500 μM lipids, 5 μM peptide) gives a local peptide concentration in the range of 2 to 4 mM which is two orders of magnitude higher than the standard concentration used for solvated peptides (40 μM), as shown in Table 2. To investigate whether the increased local concentration affects the lipopeptides' preferred conformations, CD spectra of peptide functionalized liposomes were recorded with CPeg$_4$Pn and CPeg$_{12}$Pn derivatives and compared to spectra of solvated peptides in the absence and presence of liposomes (Fig. 3). The well described helical characteristics of membrane tethered peptides E_3 and K_3 are included for comparison.[40,41,69]

A few significant effects are clearly visible. Firstly, the % H of most N-acetylated peptides did not change significantly upon a five fold concentration increase from 40 μM to 200 μM, only AcP4$_E$ tends to homooligomerize at 200 μM like AcK$_3$ (% ΔH = +20). Also, none of the P-peptides had a significant % ΔH in the
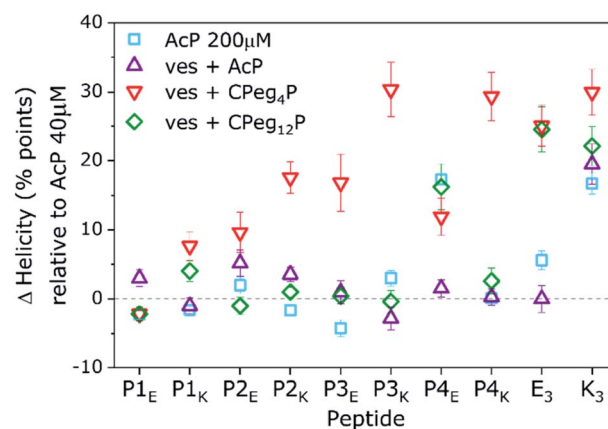

Fig. 3 Change in peptide helicity in the absence and presence of liposomes relative to helicity found for solvated peptides at 40 μM. Measured conditions: 200 μM in PBS (squares), acetylated peptides in the presence of liposomes (up-triangles) and peptides tethered to liposomes with a CPeg$_4$ anchor (down triangles) and a CPeg$_{12}$ anchor (diamonds). [Total lipid] + [AcP] = 1 mM + 40 μM. [Total lipid] + [CPegP] = 0.5 mM + 5 μM, PBS pH 7.4, 20 °C. Lipid composition = DOPC/ DOPE/cholesterol 2 : 1 : 1. Error bars represent 5% concentration deviation and spectral noise.

presence of liposomal membranes. Therefore, acetylated P-peptides do not possess spontaneous membrane interactions like AcK$_3$. Furthermore, membrane tethering of P-peptides with CPeg$_{12}$ spacers did not affect the peptide helicity except for again CPeg$_{12}$P4$_E$ (% $\Delta H = 20$). Because this % ΔH is similar to the value found for AcP4$_E$ at 200 μM we suggest that CPeg$_{12}$P4$_E$ forms homo-oligomers due to the high local concentration of lipopeptides (2 mM). Homo-oligomerisation of membrane tethered peptides was also found for CPeg$_8$E$_3$ with a % ΔH around 25. In contrast, membrane immobilization of P-peptides with the much shorter CPeg$_4$ spacer induced structural changes for all derivatives but CPeg$_4$P1$_E$. The found helicity increase shows that the limited degrees of freedom of the CPeg$_4$ spacer forces most peptides in more helical structures and only P1$_E$ was not affected by membrane immobilization. This peptide adopted random coils under all tested conditions, most likely due to its polyglutamic nature–glutamic acid accounts for 30% of the sequence and the peptide has a −10 charge at pH 7.4.

Membrane immobilized peptides can adopt two different conformations with similar overall helicities: membrane-interacting α-helices and membrane tethered homo-oligomers. These two conformations are impossible to resolve from isothermal CD spectra, but they have different unfolding behavior due to 1st and 2nd order processes.[42] Thus, thermal unfolding curves of membrane tethered CPeg$_4$Pn peptides were recorded at different concentrations to distinguish between these two secondary structures. (Fig. S7–S11†) The obtained thermal unfolding curves show distinct profiles for various peptides. Firstly, CPeg$_4$P1$_K$ and CPeg$_4$P3$_K$ show an increased helicity even at 60 °C suggesting membrane immersed conformations, because homodimers would have been mostly dissociated at this temperature.[42] As discussed above, peptide P1$_K$ is the only P-peptide with Lys residues at all e and g positions, enabling a stable membrane immersion with help of the 'snorkeling' mechanism as was reported for peptide K.[40] Secondly, CPeg$_4$P2$_E$, −P3$_E$ and −P4$_E$ show increased helicities at room temperature but similar helicities at 60 °C compared to their N-acetylated derivatives, which indicates the formation of homo-oligomers. Surprisingly, we observed a third and very unexpected structure for membrane tethered α-helical peptides at membrane functionalizations ≥2 mol%: β-sheet like structures were found for the lipopeptides CPeg$_4$2$_K$ and CPeg$_4$4$_K$ (Fig. S6†). The melting curves of these peptides support the observed β-sheet formation with a very low temperature dependency. The sequences of these two peptides do have a specific characteristic which could be stabilizing β-sheet formation at very high concentration; the hydrophobic pattern and electrostatic pattern overlap perfectly with K & I and E & N in each heptad. We did not further investigate this sequence–structure relationship since β-sheet formation only occurred at increased peptide concentrations, less relevant for membrane fusion, although concentration induced conformational changes between α-helices and β-sheets is a very interesting topic to study. Thus, membrane tethered CC peptides can adopt vastly different conformations due to high local concentration
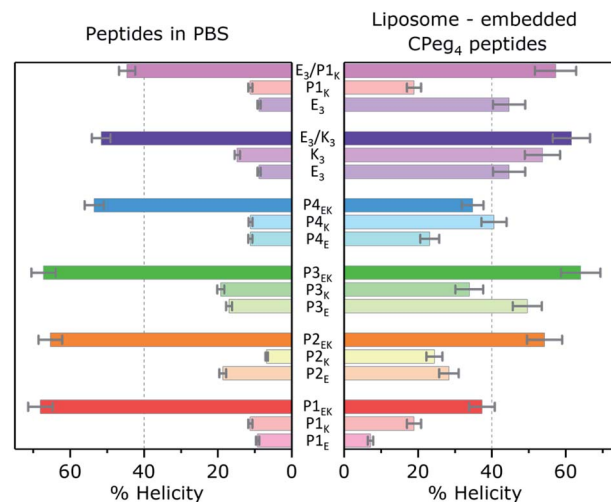

Fig. 4 Left: Helicity found for CC pairs and individual peptides in the absence of membranes, [total peptide] = 40 μM, PBS pH 7.4, at 20 °C. Right: Helicity found for CPeg$_4$Pn or CPeg$_8$E$_3$/K$_3$ membrane tethered peptides, and the equimolar mixture of liposomes bearing complementary peptides. [Total lipid] = 0.5 mM, with 1% mol lipopeptide, PBS pH 7.4, 20 °C. Lipid composition = DOPC/DOPE/cholesterol 2 : 1 : 1. Error bars represent 5% concentration deviation and spectral noise.

depending on charge and hydrophobicity patterns in the peptide sequence.

CC formation of lipopeptides

The first step of the fusion process is the docking stage, when supramolecular recognition by the fusogen forces opposing liposomes into close proximity despite the charge repulsion of their negatively charged membranes. In our model system, docking of liposomes is facilitated via CC formation of complementary peptides tethered to opposing liposomes. An
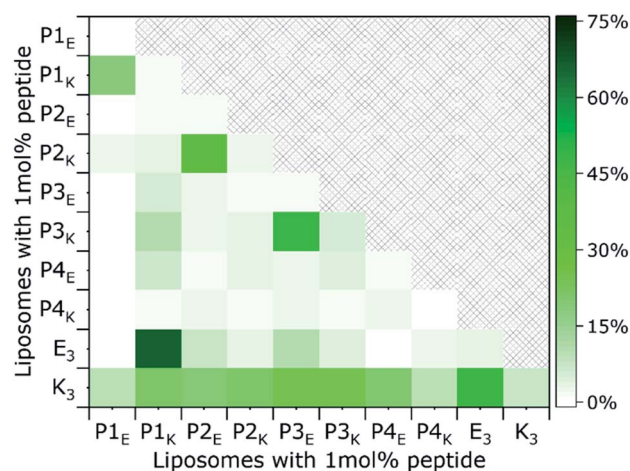

Fig. 5 Membrane fusion assay. Content mixing fusion efficiency of liposomes loaded with sulphorhodamine B (x-axis) and buffer containing liposomes (y-axis), as a function of lipopeptide derivative, after 30 min. [Total lipid] = 0.1 mM, with 1 mol% lipopeptide in PBS pH 7.4, 24 °C. Lipid composition = DOPC/DOPE/cholesterol 2 : 1 : 1.

important characteristic to quantify is the ability of the Pn_{EK} pairs to form a CC conformation and exert enough force on both liposomes to overcome their charge repulsion. Thus, liposomes functionalized with complementary peptides were mixed and the recorded helicity values before and after mixing are shown in Fig. 4 (full spectra available in Fig. S12†). The extent of CC binding of peptides tethered to opposing liposomes varied significantly between the six CC peptide pairs. Liposomes decorated with lipopeptide pairs $P2_{EK}$, $P3_{EK}$, E_3/K_3 and $E_3/P1_K$ showed strong minima at θ_{222} and θ_{208} and significant % ΔH upon mixing, demonstrating a significant coiled-coil interaction. In contrast, low helicity values (<40%) were observed for mixtures of liposomes decorated with peptide pairs $P1_{EK}$ and $P4_{EK}$ indicating the absence of strong or persistent CC interactions.

Content mixing assay. A successful liposomal fusion event is usually defined as leakage free content mixing of two liposomes. We used a quantitative content mixing assay for populations of small liposomes by encapsulating the water-soluble dye sulphorhodamine B.[36,70,71] This dye has self-quenching properties at increased concentrations, and dilution caused by fusion results in relief of self-quenching and an increase in fluorescence. Therefore, one batch of liposomes bearing peptide $CPeg_4Pn$ was loaded with 20 mM sulphorhodamine B in PBS, and mixed with peptide $CPeg_4Pn$-, $CPeg_8E_3$- or $CPeg_8K_3$-decorated buffer-containing liposomes. The fluorescence increase was followed for 30 min, after which in general a plateau was observed. In these experiments, $CPeg_4$ functionalized P-peptides and $CPeg_8$ functionalized E_3/K_3 peptides were used to account for the shorter peptide length of E_3/K_3 compared to P-peptides; also, $CPeg_8E_3/K_3$ is more fusogenic than $CPeg_4E_3/K_3$.[30] As shown in Fig. 5, fluorescence increase was only observed with a few CC peptide combinations: Efficient fusion of liposomes (>30% content mixing) was obtained when cholesterol anchored CC pairs $P2_{EK}$, $P3_{EK}$, $E_3/P1_K$, and E_3/K_3 were used as fusogen (full traces available in Fig. S13†). Liposomes functionalized with the lipopeptide pair $P1_{EK}$ or combinations of lipopeptides Pn and K_3 yielded between 10% and 25% content mixing while fusion was absent when the lipopeptide pair $P4_{EK}$

or non-complementary lipopeptides were tried as fusogens. Control experiments showed only 10% leakage for the $E_3/P1_K$ fusogen and negligible leakage for the $P2_{EK}$ and $P3_{EK}$ fusogens; and fusion between peptide functionalized liposomes and bare liposomes was absent. The negligible fluorescence increase for 75% of the tried peptide combinations and the very small amounts of leakage we previously found for the highly fusogenic E_3/K_3 pair[29,72] further show that peptide functionalized liposomes are rather stable, do not burst over the course of the experiment, and that our liposomal fusion assay does not suffer significant leakage during the actual fusion process regardless of the used peptide fusogen. Four different fusogenic effects are easily recognized: first of all, it is evident that amphipathic peptides can be fusogenic and that efficient fusion only occurs when liposomes are functionalized with complementary CC forming lipopeptides. The observed lack of fusion with $CPeg_4$-$P4_{EK}$ functionalized liposomes agrees with the inability of this complementary peptide pair to initiate even liposomal docking as shown in Fig. 3. Secondly, the negligible fusion efficiency found for non-complementary $CPeg_4Pn$ lipopeptides illustrates that a set of orthogonal CC peptides maintain their partner-selectivity even when tethered to liposomes. Thirdly, the hybrid $CPeg_8E_3/CPeg_4P1_K$ peptide pair is even more efficient in mediating fusion than the designed $CPeg_8E_3/CPeg_8K_3$ fusogen ($67 \pm 9\%$ vs. $50 \pm 5\%$ content mixing), despite its rather low K_F. And finally, the high fusogenic activity of the positively charged amphipathic K_3 peptide is evident here by the observed fusion efficiencies of $\pm20\%$ regardless of the peptide functionalization of opposing liposomes except E_3, $P1_E$ and $P4_K$.

Structure–activity relationships of peptide fusogens

Besides these four clear fusogenic effects, further analysis of the peptide structure revealed a deeper understanding of preferred peptide conformations and fusogenic efficiency as shown in Fig. 6. In general, peptide pairs with higher helicities before fusion reach higher fusion efficiencies, suggesting that fusion is enhanced by pre-formed helices and oligomer formation. This agrees with our recent finding that peptide K_3 becomes more
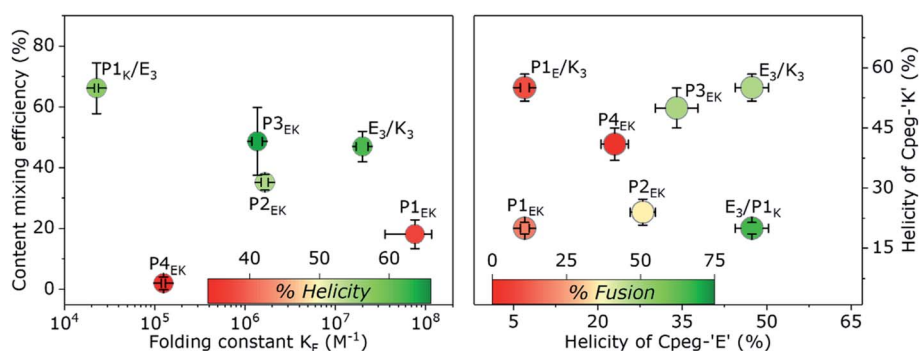

Fig. 6 Left: Content mixing efficiency of peptide fusogens in a liposomal fusion assay as a function of K_F of the peptide pair. Colours correspond to helicities of peptide functionalized liposomes after mixing and are a measure for the extent of liposomal docking. Right: Content mixing efficiency as a function of the found helicity of both membrane tethered partners before mixing. The non-fusogenic hybrid $1_E/K$ pair is shown for comparison with the highly fusogenic hybrid $E/1_K$ pair. All error bars include a 5% concentration error; K_F errors arose from the fitting procedure, % fusion errors were obtained by standard deviation with $n = 4$ and % helicity errors represent spectral noise.

fusogenic by stapling, which increased its helicity and caused CC accumulation around the fusion interface.[72] Interestingly, a reverse relationship is clearly visible between fusion efficiency and K_F of all fusogens except for P4$_{EK}$. Therefore, CC binding strength of the fusogens in our system can not be the main driving force of CC peptide mediated fusion, as was hypothesized earlier.[31]

We also hypothesized previously that the high efficacy of the E$_3$/K$_3$ fusogen is caused by the characteristic membrane destabilization of lipopeptide K$_3$.[40] The natural SNARE-protein was also shown to lower the fusion energy barriers by applying mechanical stress to the connected membranes during crucial intermediate stages.[5,73] For the CPeg$_4$Pn peptides, CD measurements suggested peptide-membrane interactions for only P1$_K$ and P3$_K$, which correlates very well with the high fusion efficiency of CPeg$_8$E$_3$/CPeg$_4$1$_K$ and CPeg$_4$P3$_E$/CPeg$_4$P3$_K$ supporting this hypothesis. These two peptides, P1$_K$ and P3$_K$, are the only P-peptides having lysine residues at the e and g positions of the 2nd and 3rd heptad, suggesting that positive charges at these positions enhance the membrane interaction and the fusogenic activity.

Since the P2$_{EK}$ fusogen did not interact with its supporting membranes it is very likely that the fusion process with these peptides is mainly driven by the force released upon CC formation of the fusogen. The very close apposition of both liposomes in the docking state initiates the fusion process without further influence of the fusogen. This agrees with the moderate 40% fusion efficiency reached after 30 min. Many other synthetic fusogens who typically did not disturb their supporting membranes were found to solely facilitate docking of liposomes and never reached more than 40% fusion efficiency under similar conditions.[44] This suggests that higher fusion efficiencies can only be reached with additional membrane disturbing effects caused by, for instance, membrane composition,[74] or peptide–membrane interactions. However, the fusogenic efficacy of membrane disturbing peptides can be hampered by a suboptimal membrane anchoring as even the highly fusogenic E$_3$/K$_3$ peptide pair could only reach 20% fusion efficiency when DOPE was used as the membrane anchor or when cholesterol-peg$_4$ linkers were applied.[30]

Comparison of the CPeg$_4$P1$_E$/CPeg$_4$P1$_K$ and CPeg$_8$E$_3$/CPeg$_4$P1$_K$ pairs revealed the remarkable influence of the partner-peptide on the efficiency of the fusion process. Both 'E' like derivatives, CPeg$_4$P1$_E$ and CPeg$_8$E$_3$, are negatively charged peptides but their preferred secondary structures differ vastly. CD spectra of CPeg$_4$P1$_E$ showed a random coil conformation while CPeg$_8$E$_3$ was found in a predominantly homodimeric CC conformation at room temperature.[41] The peptide helicity increased to only 40% upon mixing of CPeg$_4$P1$_E$ and CPeg$_4$P1$_K$ functionalized liposomes while a mixture of CPeg$_8$E$_3$/CPeg$_4$P1$_K$ functionalized liposomes showed 60% helicity. The larger helicity increase of the E$_3$/P1$_K$ fusogen seemed to contradict its much lower binding strength compared to P1$_{EK}$, but we suggest that the highly ordered structure of CPeg$_8$E$_3$ over CPeg$_4$P1$_E$ increased the peptide availability and enhanced the CC formation despite the lower K_F. Secondly, fusion efficiencies of the 4 possible lipopeptide combinations follow the order E$_3$/P1$_K$ > E$_3$/

K$_3$ > P1$_{EK}$ > P1$_E$/K$_3$. Thus exchanging the 'E' peptide from E$_3$/P1$_K$ to P1$_E$/P1$_K$ has a bigger inhibitive effect on fusion than exchanging the 'K' peptide from E$_3$/P1$_K$ to E$_3$/K$_3$, illustrating the importance of pre-fusion CPeg$_8$E$_3$ homodimer formation. Furthermore, the absence of any significant interaction between P1$_E$ and K$_3$ (the oppositely charged hypothetical hybrid pair) shows that the hybrid interaction is not primarily based on electrostatic attractions and CC formation, corroborating the conformation bias of prefolded E$_3$ homodimers. Thirdly, visible aggregates of liposomes were only observed when CPeg$_8$E$_3$/CPeg$_4$P1$_K$ was used as the fusogen, as was also observed for CPeg$_{12}$E$_3$/CPeg$_{12}$K$_3$ (ref. 30) (Fig. S14†). However, aggregation of liposomes was not observed when CPeg$_4$2$_{EK}$, CPeg$_4$3$_{EK}$ and other pairs were used as fusogens. If this liposomal aggregation was only caused by CC formation, aggregation should have been visible for at least the P2$_{EK}$ and P3$_{EK}$ lipopeptide pairs since they have a higher K_F and a similar %H upon liposomal docking as CPeg$_8$E$_3$/CPeg$_4$P1$_K$. As the affinity of E$_3$/P1$_K$ is the lowest among all used peptide fusogens, this is highly unlikely and we suggest another explanation of this particular effect. The found K_F of E$_3$/P1$_K$ in solution is 2.3×10^4 M^{-1}, which correspond to a folded fraction (α) of 0.5 at 24 °C and 100 μM. Although peptide characteristics are affected by membrane tethering, we assume that the CC interaction of CPeg$_8$E$_3$/CPeg$_4$P1$_K$ is sufficiently strong to induce liposomal docking (as shown in Fig. 4), but too weak to remain fully folded after the fusion event. We found previously that the CPeg$_{12}$E$_3$/CPeg$_{12}$K$_3$ fusogen was able to mediate multiple rounds of fusion due to CC disassembly after a completed fusion event; because peptides need to be available to initiate consecutive docking states. So we suggest that the low K_F of E$_3$/P1$_K$ causes partial CC disassembly after a completed fusion event, increasing the peptides' chance to initiate a next round of fusion. Also, the fluorescence increase showed no plateau like other fusogens, suggesting that the fusion process does not stop after one round. Therefore, we theorize that the very high fusion efficiency of this hybrid peptide pair is caused by the unique combination of an enhanced availability of the homodimer CPeg$_8$E$_3$, the apparent membrane interaction of CPeg$_4$P1$_K$ and the well-balanced strength of the heterodimeric CC interactions, which all can be probed in further studies.

Conclusions

This study demonstrated the fusogenic activity of a small library of lipidated orthogonal CC peptides. Interactome analysis of the four Pn_{EK} pairs with the known CC pair E$_3$/K$_3$ revealed one major cross-pair interaction between P1$_K$ and E$_3$. All six CC interactions were found to be heterodimeric CCs with K_F's ranging from 10^4 M^{-1} to 10^8 M^{-1}. The hybrid CC interaction E$_3$/P1$_K$ is destabilized by two Asn–Ile mismatches, which are rare for stable CC conformations, but the associated energy penalty is in agreement with literature. However, MD simulations suggested the formation of a parallel heterodimer with buried Lysines and fully solvated Asn residues, resulting in a shifted heptad repeat register.

Efficient content mixing was found between liposomes functionalized with the lipopeptide pairs P2$_{EK}$, P3$_{EK}$, and E$_3$/

$P1_K$. Examination of peptide structure and fusogenic efficiency revealed that lower K_Fs enhance the fusion process to a certain extent, contrary to earlier hypotheses, most likely by increasing peptide availability for consecutive fusion events. Furthermore, fusogens with explicit asymmetric roles were found to be highly fusogenic. The roleplay of the fusogen is defined by peptide conformations of membrane tethered peptides before the fusion event. The preferred conformation depends on the precise patterns of electrostatic and hydrophobic residues and the spacer length; in this set of eight similar $CPeg_4Pn$ peptides, we found a random coil ($P1_E$), three CC oligomer forming peptides ($P2_E$, $P3_E$, $P4_E$), two membrane interacting α-helical peptides ($P1_K$, $P3_K$), and surprisingly, two peptides in a β-sheet conformation ($P2_K$, $P4_K$). Notably, $CPeg_{12}$ spacers were in general too long to curtail the peptides' structural freedom. Thus, the roleplay could be clearly identified for the efficient fusogens $P3_{EK}$ and $E_3/P1_K$ (and the described E_3/K_3): An 'active' role with a membrane interacting peptide 'K', and a 'passive' role with a highly accessible and very helical peptide 'E' homodimer. These distinct peptide conformations were not observed for fusogen $P2_{EK}$. We assume this peptide pair mediated fusion by 'forcing' opposing liposomes together, thereby reaching lesser fusion efficiencies than the roleplaying peptides. The peptide pairs $P1_{EK}$ and $P4_{EK}$ were found to be only slightly fusogenic because they were not able to efficiently form CCs between opposing liposomes and initiate their fusion.

The high efficiency and the absence of non-specific fusion events of the $P2_{EK}$, $P3_{EK}$, and $E_3/P1_K$ fusogens makes these peptides useful candidates for the development of both programmable liposomal fusion assays[13] and partner specific liposome–cell fusion assays.[35,36] Furthermore, this research bridged the gap between peptide mediated liposomal fusion model systems and supramolecular self-assembly of peptide functionalized building blocks and aids *de novo* peptide design by unravelling multiple important sequence–structure relationships of CC-forming peptides.

Data availability

Detailed experimental protocols, CD spectra, Molecular Dynamic simulation analysis, and supplementary figures are provided in the ESI.†

Author contributions

GAD and AK designed the study. GAD, MS and PE synthesized the peptides. GAD conducted CD spectroscopy and content mixing experiments. PE carried out CD spectroscopy supervised by GAD. MS performed leakage control experiments. AS performed MD simulations supervised by GJAS. GAD wrote the manuscript with input from GJAS, ALB and AK.

Conflicts of interest

There are no conflicts to declare.

Notes and references

1 R. Jahn and H. Grubmüller, Membrane fusion, *Curr. Opin. Cell Biol.*, 2002, **14**, 488–495.

2 Y. A. Chen and R. H. Scheller, SNARE-mediated membrane fusion, *Nat. Rev. Mol. Cell Biol.*, 2001, **2**, 98–106.

3 R. Jahn and R. H. Scheller, SNAREs–engines for membrane fusion, *Nat. Rev. Mol. Cell Biol.*, 2006, **7**, 631–643.

4 H. J. Risselada and H. Grubmuller, How SNARE molecules mediate membrane fusion: recent insights from molecular simulations, *Curr. Opin. Struct. Biol.*, 2012, **22**, 187–196.

5 J. Han, K. Pluhackova and R. A. Bockmann, The Multifaceted Role of SNARE Proteins in Membrane Fusion, *Front. Membr. Physiol. Membr. Biophys.*, 2017, **8**, 5.

6 G. Stengel, R. Zahn and F. Höök, DNA-Induced Programmable Fusion of Phospholipid Vesicles, *J. Am. Chem. Soc.*, 2007, **129**, 9584–9585.

7 G. Stengel, L. Simonsson, R. A. Campbell and F. Höök, Determinants for Membrane Fusion Induced by Cholesterol-Modified DNA Zippers, *J. Phys. Chem. B*, 2008, **112**, 8264–8274.

8 Y.-H. M. Chan, B. Van Lengerich and S. G. Boxer, Lipid-anchored DNA mediates vesicle fusion as observed by lipid and content mixing, *Biointerphases*, 2008, **3**, FA17.

9 Y. H. Chan, B. van Lengerich and S. G. Boxer, Effects of linker sequences on vesicle fusion mediated by lipid-anchored DNA oligonucleotides, *Proc. Natl. Acad. Sci. U. S. A.*, 2009, **106**, 979–984.

10 U. Jakobsen and S. Vogel, DNA-Controlled Assembly of Liposomes in Diagnostics, *Methods Enzymol.*, 2009, **464**, 233–248.

11 Z. Meng, *et al.*, Efficient Fusion of Liposomes by Nucleobase Quadruple-Anchored DNA, *Chem.–Eur. J.*, 2017, **23**, 9391–9396.

12 P. M. G. Löffler, et al., A DNA-Programmed Liposome Fusion Cascade, *Angew. Chem., Int. Ed.*, 2017, **56**, 13228–13231.

13 A. Rabe, P. M. G. Löffler, O. Ries and S. Vogel, Programmable fusion of liposomes mediated by lipidated PNA, *Chem. Commun.*, 2017, **53**, 11921–11924.

14 O. Ries, P. M. G. Löffler and S. Vogel, Convenient synthesis and application of versatile nucleic acid lipid membrane anchors in the assembly and fusion of liposomes, *Org. Biomol. Chem.*, 2015, **13**, 9673–9680.

15 O. Ries, P. M. G. Löffler, A. Rabe, J. J. Malavan and S. Vogel, Efficient liposome fusion mediated by lipid-nucleic acid conjugates, *Org. Biomol. Chem.*, 2017, **15**, 8936–8945.

16 A. S. Lygina, K. Meyenberg, R. Jahn and U. Diederichsen, Transmembrane domain peptide/peptide nucleic acid hybrid as a model of a snare protein in vesicle fusion, *Angew. Chem., Int. Ed.*, 2011, **50**, 8597–8601.

17 A. Kashiwada, K. Matsuda, T. Mizuno and T. Tanaka, Construction of a pH-responsive artificial membrane fusion system by using designed coiled-coil polypeptides, *Chem.–Eur. J.*, 2008, **14**, 7343–7350.

18 K. Meyenberg, A. S. Lygina, G. van den Bogaart, R. Jahn and U. Diederichsen, SNARE derived peptide mimic inducing membrane fusion, *Chem. Commun.*, 2011, **47**, 9405–9407.

19 M. Rauschenberg, S. Bomke, U. Karst and B. J. Ravoo, Dynamic Peptides as Biomimetic Carbohydrate Receptors, *Angew. Chem., Int. Ed.*, 2010, **49**, 7340–7345.

20 F. Mazur and R. Chandrawati, Peptide-Mediated Liposome Fusion as a Tool for the Detection of Matrix Metalloproteinases, *Adv. Biosyst.*, 2019, **3**, 1–8.

21 P. M. G. Löffler, *et al.*, Lipidated Polyaza Crown Ethers as Membrane Anchors for DNA-Controlled Content Mixing between Liposomes, *Sci. Rep.*, 2019, **9**, 1–11.

22 A. Richard, *et al.*, Fusogenic supramolecular vesicle systems induced by metal ion binding to amphiphilic ligands, *Proc. Natl. Acad. Sci. U. S. A.*, 2004, **101**, 15279–15284.

23 Y. Gong, Y. Luo and D. Bong, Membrane activation: selective vesicle fusion via small molecule recognition, *J. Am. Chem. Soc.*, 2006, **128**, 14430–14431.

24 A. Kashiwada, M. Tsuboi and K. Matsuda, Target-selective vesicle fusion induced by molecular recognition on lipid bilayers, *Chem. Commun.*, 2009, 695–697.

25 A. Kashiwada, M. Tsuboi, T. Mizuno, T. Nagasaki and K. Matsuda, Target-selective vesicle fusion system with pH-selectivity and responsiveness, *Soft Matter*, 2009, **5**, 4719–4725.

26 A. Kashiwada, *et al.*, Design and Characterization of Endosomal-pH-Responsive Coiled Coils for Constructing an Artificial Membrane Fusion System, *Chem.–Eur. J.*, 2011, **17**, 6179–6186.

27 V. Marchi-Artzner, *et al.*, Selective adhesion, lipid exchange and membrane-fusion processes between vesicles of various sizes bearing complementary molecular recognition groups, *ChemPhysChem*, 2001, **2**, 367–376.

28 M. M. Ma and D. Bong, Controlled Fusion of Synthetic Lipid Membrane Vesicles, *Acc. Chem. Res.*, 2013, **46**, 2988–2997.

29 F. Versluis, *et al.*, In situ modification of plain liposomes with lipidated coiled coil forming peptides induces membrane fusion, *J. Am. Chem. Soc.*, 2013, **135**, 8057–8062.

30 G. A. Daudey, H. R. Zope, J. Voskuhl, A. Kros and A. L. Boyle, Membrane-Fusogen Distance Is Critical for Efficient Coiled-Coil-Peptide-Mediated Liposome Fusion, *Langmuir*, 2017, **33**, 12443–12452.

31 T. Zheng, *et al.*, Controlling the rate of coiled coil driven membrane fusion, *Chem. Commun.*, 2013, **49**, 3649–3651.

32 F. Versluis, J. Dominguez, J. Voskuhl and A. Kros, Coiled-coil driven membrane fusion: zipper-like vs. non-zipper-like peptide orientation, *Faraday Discuss.*, 2013, **166**, 349–359.

33 T. Zheng, *et al.*, A non-zipper-like tetrameric coiled coil promotes membrane fusion, *RSC Adv.*, 2016, **6**, 7990–7998.

34 N. S. A. Crone, D. Minnee, A. Kros and A. L. Boyle, Peptide-mediated liposome fusion: The effect of anchor positioning, *Int. J. Mol. Sci.*, 2018, **19**, 211.

35 H. R. Zope, *et al.*, In vitro and in vivo supramolecular modification of biomembranes using a lipidated coiled-coil motif, *Angew. Chem., Int. Ed.*, 2013, **52**, 14247–14251.

36 J. Yang, *et al.*, Drug Delivery via Cell Membrane Fusion Using Lipopeptide Modified Liposomes, *ACS Cent. Sci.*, 2016, **2**, 621–630.

37 N. L. Mora, *et al.*, Controlled Peptide-Mediated Vesicle Fusion Assessed by Simultaneous Dual-Colour Time-Lapsed Fluorescence Microscopy, *Sci. Rep.*, 2020, **10**, 1–13.

38 L. Kong, Q. Chen, F. Campbell, E. Snaar-Jagalska and A. Kros, Light-Triggered Cancer Cell Specific Targeting and Liposomal Drug Delivery in a Zebrafish Xenograft Model, *Adv. Healthcare Mater.*, 2020, **9**, 1901489.

39 M. Rabe, C. Schwieger, H. R. Zope, F. Versluis and A. Kros, Membrane Interactions of Fusogenic Coiled-Coil Peptides: Implications for Lipopeptide Mediated Vesicle Fusion, *Langmuir*, 2014, **30**, 7724–7735.

40 M. Rabe, *et al.*, A Coiled-Coil Peptide Shaping Lipid Bilayers upon Fusion, *Biophys. J.*, 2016, **111**, 2162–2175.

41 G. A. Daudey, C. Schwieger, M. Rabe and A. Kros, Influence of Membrane–Fusogen Distance on the Secondary Structure of Fusogenic Coiled Coil Peptides, *Langmuir*, 2019, **35**, 5501–5508.

42 M. Rabe, H. R. Zope and A. Kros, Interplay between Lipid Interaction and Homo-coiling of Membrane-Tethered Coiled-Coil Peptides, *Langmuir*, 2015, **31**, 9953–9964.

43 A. Koukalová, *et al.*, Distinct roles of SNARE-mimicking lipopeptides during initial steps of membrane fusion, *Nanoscale*, 2018, **10**, 19064–19073.

44 H. R. Marsden, I. Tomatsu and A. Kros, Model systems for membrane fusion, *Chem. Soc. Rev.*, 2011, **40**, 1572–1585.

45 C. Negron and A. E. Keating, A set of computationally designed orthogonal antiparallel homodimers that expands the synthetic coiled-coil toolkit, *J. Am. Chem. Soc.*, 2014, **136**, 16544–16556.

46 J. M. Fletcher, *et al.*, A Basis Set of de Novo Coiled-Coil Peptide Oligomers for Rational Protein Design and Synthetic Biology, *ACS Synth. Biol.*, 2012, **1**, 240–250.

47 C. Aronsson, *et al.*, Self-sorting heterodimeric coiled coil peptides with defined and tuneable self-assembly properties, *Sci. Rep.*, 2015, **5**, 14063.

48 R. O. Crooks, D. Baxter, A. S. Panek, A. T. Lubben and J. M. Mason, Deriving Heterospecific Self-Assembling Protein-Protein Interactions Using a Computational Interactome Screen, *J. Mol. Biol.*, 2016, **428**, 385–398.

49 R. O. Crooks, A. Lathbridge, A. S. Panek and J. M. Mason, Computational Prediction and Design for Creating Iteratively Larger Heterospecific Coiled Coil Sets, *Biochemistry*, 2017, **56**, 1573–1584.

50 E. H. C. Bromley, R. B. Sessions, A. R. Thomson and D. N. Woolfson, Designed α-Helical Tectons for Constructing Multicomponent Synthetic Biological Systems, *J. Am. Chem. Soc.*, 2009, **131**, 928–930.

51 A. W. Reinke, R. A. Grant and A. E. Keating, A Synthetic Coiled-Coil Interactome Provides Heterospecific Modules for Molecular Engineering, *J. Am. Chem. Soc.*, 2010, **132**, 6025–6031.

52 M. L. Diss and A. J. Kennan, Orthogonal Recognition in Dimeric Coiled Coils via Buried Polar-Group Modulation, *J. Am. Chem. Soc.*, 2008, **130**, 1321–1327.

53 H. Gradišar and R. Jerala, De novo design of orthogonal peptide pairs forming parallel coiled-coil heterodimers, *J. Pept. Sci.*, 2011, **17**, 100–106.

54 N. J. Greenfield, Using circular dichroism collected as a function of temperature to determine the thermodynamics of protein unfolding and binding interactions, *Nat. Protoc.*, 2006, **1**, 2527–2535.

55 N. J. Greenfield, Methods to estimate the conformation of proteins and polypeptides from circular dichroism data, *Anal. Biochem.*, 1996, **235**, 1–10.

56 E. Lacroix, A. R. Viguera and L. Serrano, Elucidating the folding problem of α-helices: local motifs, long-range electrostatics, ionic-strength dependence and prediction of NMR parameters 1 1Edited by A. R. Fersht, *J. Mol. Biol.*, 1998, **284**, 173–191.

57 M. Rabe, A. Boyle, H. R. Zope, F. Versluis and A. Kros, Determination of Oligomeric States of Peptide Complexes Using Thermal Unfolding Curves, *Biopolymers*, 2015, **104**, 65–72.

58 R. M. Fesinmeyer, E. S. Peterson, R. B. Dyer and N. H. Andersen, Studies of helix fraying and solvation using 13 C′ isotopomers, *Protein Sci.*, 2005, **14**, 2324–2332.

59 C. Dalgicdir, C. Globisch, C. Peter and M. Sayar, Tipping the Scale from Disorder to Alpha-helix: Folding of Amphiphilic Peptides in the Presence of Macroscopic and Molecular Interfaces, *PLoS Comput. Biol.*, 2015, **11**, e1004328.

60 K. J. Lumb and P. S. Kim, A Buried Polar Interaction Imparts Structural Uniqueness in a Designed Heterodimeric Coiled Coil, *Biochemistry*, 1998, **37**, 13042.

61 M. G. Oakley and P. S. Kim, A Buried Polar Interaction Can Direct the Relative Orientation of Helices in a Coiled Coil, *Biochemistry*, 1998, **37**, 12603–12610.

62 D. L. Akey, V. N. Malashkevich and P. S. Kim, Buried Polar Residues in Coiled-Coil Interfaces, *Biochemistry*, 2001, **40**, 6352–6360.

63 D. L. Lee, S. Ivaninskii, P. Burkhard and R. S. Hodges, Unique stabilizing interactions identified in the two-stranded α-helical coiled-coil: Crystal structure of a cortexillin I/GCN4 hybrid coiled-coil peptide, *Protein Sci.*, 2003, **12**, 1395–1405.

64 M. S. Sunitha, A. G. Nair, A. Charya, K. Jadhav and S. Mukhopadhyay, Structural attributes for the recognition of weak and anomalous regions in coiled-coils of myosins and other motor proteins, *BMC Res. Notes*, 2012, **5**, 530.

65 F. Thomas, A. Niitsu, A. Oregioni, G. J. Bartlett and D. N. Woolfson, Conformational Dynamics of Asparagine at Coiled-Coil Interfaces, *Biochemistry*, 2017, **56**, 6544–6554.

66 A. Acharya, S. B. Ruvinov, J. Gal, J. R. Moll and C. Vinson, A heterodimerizing leucine zipper coiled coil system for examining the specificity of a position interactions: Amino acids I, V, L, N, A, and K, *Biochemistry*, 2002, **41**, 14122–14131.

67 A. Acharya, V. Rishi and C. Vinson, Stability of 100 Homo and Heterotypic Coiled-Coil a-a ′ Pairs for Ten Amino Acids, *Biochemistry*, 2006, **34**, 11324–11332.

68 J. Walshaw and D. N. Woolfson, SOCKET: a program for identifying and analysing coiled-coil motifs within protein structures, *J. Mol. Biol.*, 2001, **307**, 1427–1450.

69 P. Kumar, *et al.*, Coiled-coil formation of the membrane-fusion K/E peptides viewed by electron paramagnetic resonance, *PLoS One*, 2018, **13**, e0191197.

70 M. Kyoung, *et al.*, In vitro system capable of differentiating fast Ca2+-triggered content mixing from lipid exchange for mechanistic studies of neurotransmitter release, *Proc. Natl. Acad. Sci. U. S. A.*, 2011, **108**, E304–E313.

71 B. S. Stratton, *et al.*, Cholesterol Increases the Openness of SNARE-Mediated Flickering Fusion Pores, *Biophys. J.*, 2016, **110**, 1538–1550.

72 N. S. A. Crone, A. Kros and A. L. Boyle, Modulation of Coiled-Coil Binding Strength and Fusogenicity through Peptide Stapling, *Bioconjugate Chem.*, 2020, **31**, 834–843.

73 J. Rizo and J. Xu, The Synaptic Vesicle Release Machinery, *Annu. Rev. Biophys.*, 2015, **44**, 339–367.

74 R. Kolašinac, C. Kleusch, T. Braun, R. Merkel and A. Csiszár, Deciphering the functional composition of fusogenic liposomes, *Int. J. Mol. Sci.*, 2018, **19**, 346.